In Silico Investigation of the Functional Effects of KCNQ1-G269S Mutation in Human Ventricles

Haibo Ni, Wei Wang, Erick Andres Perez Alday, Henggui Zhang

Biological Physics Group, Department of Physics and Astronomy
University of Manchester, Manchester, United Kingdom

Abstract

A recent study identified a loss-in-function mutation KCNQ1-G269S in long-QT patients who remained asymptomatic at rest but exhibited prolonged QT intervals after exercise, showing loss-of-function and blunted adrenergic activation in the slow component of delayed rectifier K^+ current (I_{Ks}). The aim of this study was to evaluate the functional effects of the mutation in human ventricles through computer modelling. The O'Hara-Rudy model of human ventricular cells was modified to incorporate an updated model of I_{Ks} and an adrenergic activation model. The single cell models were then incorporated into a 1D strand model to quantify the effects of the mutation on tissue vulnerability in genesis of uni-directional conduction block. Using a 3D anatomical model of human ventricles and torso model, effects of the mutation on ventricular electrical activities and electrocardiograms (ECG) were simulated. It was shown that the mutation exerted moderate prolongations to action potential duration (APD) in the absence of adrenergic stimulation, and slightly increased the tissue vulnerability to produce unidirectional conduction block. These effects were much more pronounced after adrenergic stimulation. Simulated ECGs revealed moderate and severe QT prolongations for at rest and after exercise conditions respectively, which matched the clinical data. Our simulations provide insights into the pathological mechanisms of the KCNQ1-G269S mutation.

1. Introduction

Long QT syndrome (LQTS) manifests abnormal prolongations of QT interval on the electrocardiogram (ECG). Numerous genetic mutations are found to be responsible for a number of subtypes of LQTS, among which LQT1 is most prevalent [1,2]. Mutations in KCNQ1 encoding the alpha subunit of I_{Ks} are the most common cause of LQT1 [1–3]. I_{Ks} is a major repolarisation current after the plateau phase of action potentials in ventricular myocytes [2]. Upon adrenergic stimulation, I_{Ks} is vital in counterbalancing an increased activity in the L-type calcium current (I_{CaL}) [2]. A recent study identified a moderate loss-of-function mutation KCNQ1-G269S in a patient with LQTS. The patient remained asymptomatic during rest, but exhibited prolonged QT intervals after exercise [2]. The compromised adrenergic activation of I_{Ks} due to the G269S mutation was proposed to underlie the symptom. However, the exact mechanism is unclear yet. In this study, we used computational models to investigate the functional impact of the mutation on human ventricular action potentials, tissue's vulnerability of producing unidirectional conduction block of of excitation waves, and QT intervals from ECGs.

2. Methods

The WT and KCNQ1-G269S I_{Ks} was modelled based on the original I_{Ks} formulation of O'Hara *et al*. [4], which was updated to better describe the experimental data on steady-state activation and kinetics [2] (**Figure 1**). As compared to WT condition, both WT-G269S and G269S variants exhibit right-shifted steady-state activation and faster deactivation, showing loss-of-function in I_{Ks}.

The ionic models of I_{Ks} were introduced into the -Rudy model (ORd) [4] to simulate human ventricular action potentials. To model the adrenergic stimulation effects on the ventricular myocytes, we adapted the model used in O'Hara *et al*. [3] and Lee *et al*. [5] with further modifications to consider its effects on I_{CaL} and I_{Ks}. A saturating concentration of isoprenaline (ISO, 1 μM) was applied to simulate the adrenergic stimulation. The effects of ISO on I_{Ks} were modelled as shown in Table 1, where blunted adrenergic activation of I_{Ks} was considered.

A 1D strand model of transmural human ventricular wedge was used to investigate tissue vulnerability to abnormal conductions [6]. By using S1-S2 stimulus protocol, the vulnerability window was quantified as the temporal window of S2 leading to unidirectional conduction. We further simulated the effect of mutations on electrical activities of the ventricles at organ level using a 3D human ventricular model with realistic structure and myofibre orientations [6], which was then placed into our human torso model [7] to obtain ECGs.

Table 1. Modelling effects of adrenergic activation on I_{Ks}

Effects	WT	Mutations
Steady-state activation $V_{1/2}$ shifted to the left by:	7 mV [1]	2.8 mV
Activation time constant	τ_{x1}×0.6 [8]	τ_{x1}×0.84
Channel conductance	×3.2 [3]	×1.88

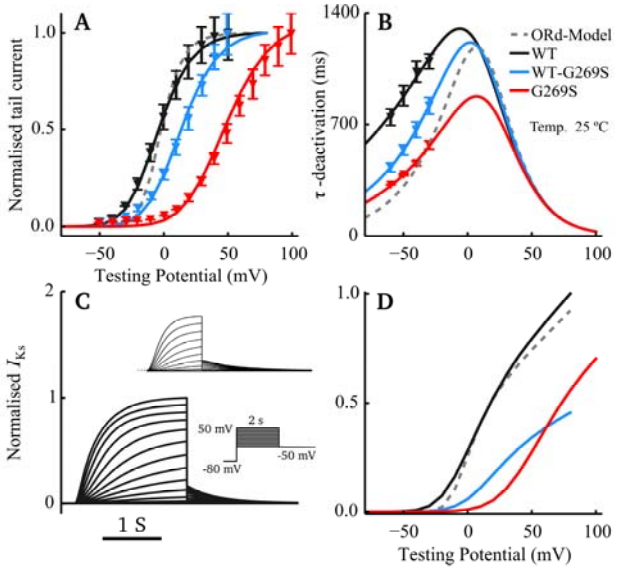

Figure 1. Simulated I_{Ks} as compared to experimental data on WT and mutation. (A) Normalised peak tail current; (B) Time constant of deactivation; (C) Current traces from voltage clamp; insert: experimental traces and voltage clamp protocol; (D) End step current-voltage relationship. The experimental data were from [2].

3. Results

3.1. Effects of KCNQ1-G269S on action potential durations

Action potential duration at 90% repolarisation (APD_{90}) was moderately prolonged by both mutants under control conditions without ISO (**Figure 2**). At a basic cycle length (BCL) of 1000 ms, APD_{90} was prolonged by 14 ms in endocardium cells (ENDO), 10 ms in epicardium cells (EPI) and 26 ms in mid-myocardial cells (MCELL) by G269S. The heterozygous mutation WT-G269S produced slightly smaller prolongations despite a significantly higher I_{Ks} current density than G269S. At a higher pacing rate (BCL = 500 ms), the APDs were lengthened by about the same amount (**Figure 2**). Moreover, the mutants also increased APD differences among the transmural cell types, as the MCELL-EPI APD difference was 108, 121 and 134 ms for WT, WT-G269S and G269S, respectively.

In the presence of ISO, the prolongations in APD_{90} by the mutations were much more pronounced. At a BCL of 1000 ms, APD_{90} was lengthened by 24 ms in ENDO, 21 ms in EPI, and 84 ms in MCELL for WT-G269S. For G269S, the prolongations were 27 and 24 ms in ENDO and EPI, respectively. Stable early after-depolarisations (EADs) were observed in the MCELL for mutant G269S, with a profound prolongation of 274 ms in APD_{90}. Furthermore, at a BCL of 500 ms, APD_{90} was prolonged by 24 ms in ENDO, 23 ms in EPI, and 51 ms in MCELL with the mutant WT-G269S, and by 28 ms in ENDO, 26 ms in EPI, and 61 ms in MCELL for G269S. EADs were not observed at this pacing rate. Similarly, the regional APD difference was also augmented by the mutants in the presence of ISO (BCL = 1000 ms: 101 vs 164 vs 350 ms; BCL = 500 ms: 76 vs 104 vs 111 ms for WT, WT-G269S and G269S, respectively).

We further investigated the role of impaired adrenergic activation of I_{Ks} in WT-G269S and G269S by restoring normal responsiveness of adrenergic activation to the mutations. Consequently, the effect of mutations on the APD of ENDO and EPI cells was slightly attenuated with normal adrenergic activation (by 6 ms for WT-G269S, 3 ms for G269S). In MCELL, restoring normal adrenergic activation function to G269S did not abolish EADs at BCL = 1000 ms, and exhibited 9 ms attenuation to APD prolongation at BCL = 500 ms. Restoring normal adrenergic activation to WT-G269S mediated larger abbreviation in prolongation effect in MCELL (by 32 ms for BCL = 1000 ms, and 13 ms for BCL = 500 ms). The contributions of blunted adrenergic activation of I_{Ks} by these mutations were quantified as the percentage reduction in APD prolongation by restoring full adrenergic activation to the corresponding mutation (**Figure 3**). Overall, the impaired adrenergic activation of I_{Ks} by the mutations accounts for more than 20% for WT-G269S and 10% for G269S. These results suggest that the effects of these mutations on APD after adrenergic stimulation could be primarily due to loss-in-function in I_{Ks}, and that blunted adrenergic activation also contributes to the profound APD prolongation but to a less extent.

3.2. Effects of KCNQ1-G269S on tissue vulnerability window

Tissue vulnerability to the genesis of unidirectional conduction in response to a premature stimulus applied to the refractory tail of a conditioning excitation was promoted by the mutations (**Figure 4**). Under the control condition, both mutations delayed the occurrence of the temporal vulnerable window (VW); the measured width of VW at the MCELL/EPI junction was much wider than that at ENDO/MCELL junction primarily owing to a more profound APD heterogeneity between MCELL and EPI under all conditions. Moreover, the widths of VW were slightly increased at the MCELL/EPI junction but

not at the ENDO/MCELL junction. Following the application of ISO, the VWs at ENDO/MCELL junction were almost diminished for WT and WT-G269S, whereas it was increased to 11 ms for G269S; at the MCELL-EPI junction, the occurrences of VWs were delayed, accompanied by an increase in widths (by 4 ms) by the mutants.

3.3. Effects of KCNQ1-G269S on QT intervals

The activation time (AT) and repolarisation time (RT) were acquired from our realistic 3D human ventricle model, showing that RT was delayed by the mutants in the absence of noticeable alterations to AT.

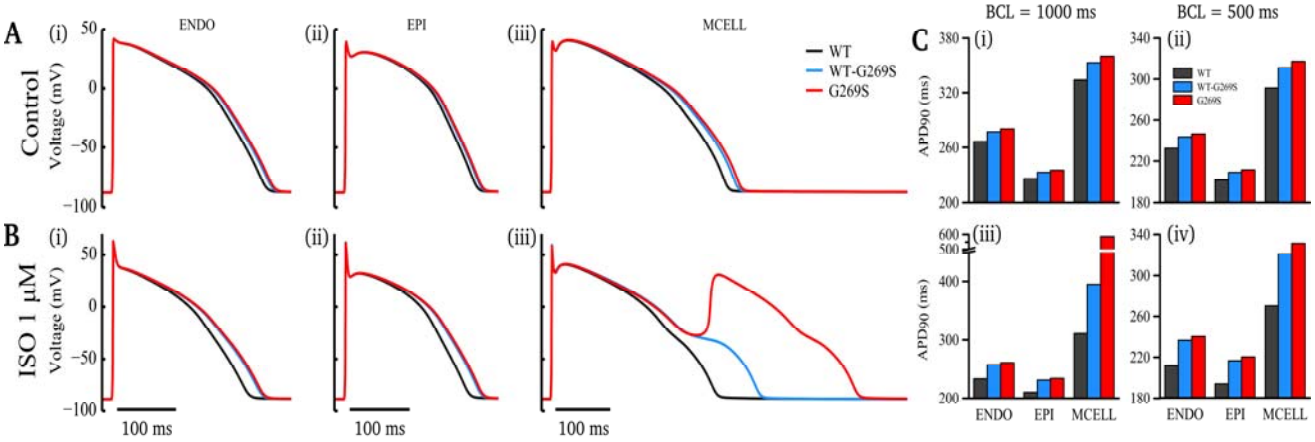

Figure 2. Effects of WT-G269S and G269S on action potentials of endocardium (ENDO), epicardium (EPI), and mid-layer cells (MCELL). A comparison in AP was made between control conditions (Ai-iii) and after application of ISO (Bi-iii) in different regional cells. Panel C summarized the APD of WT and mutants at a resting pacing rate (BCL = 1000 ms, Ci, Ciii), and a faster pacing rate (BCL = 500 ms, Cii, Civ). In panels A and B, BCL = 1000 ms.

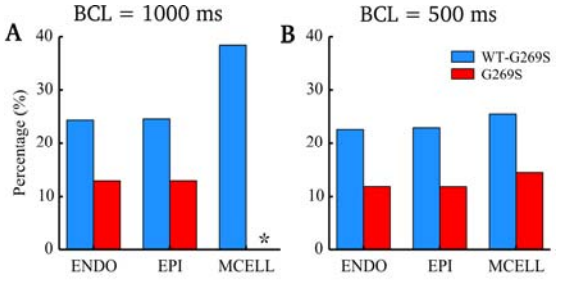

Figure 3. The percentage reduction in APD prolongation by restoring full adrenergic activation to the mutants.

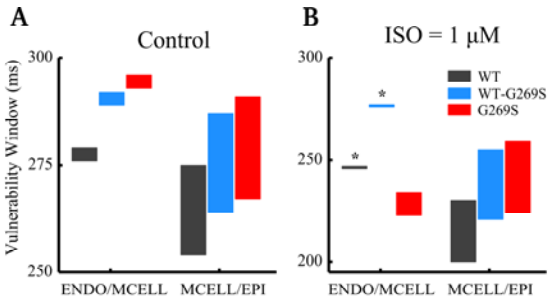

Figure 4. Effects of mutations on the tissue VW to initiating unidirectional conduction simulated from a one-dimensional strand model. S1 = 500 ms. S2 stimuli were applied to the ENDO/MCELL and MCELL/EPI junctions. * indicates where the VW was diminished.

Consequently, the activation repolarisation interval was prolonged by the mutants.

Additionally, lead II from the simulated ECGs was analysed, and QT intervals were quantified (**Figure 5**). At rest, the WT model produced a QTc of 396 ms. Both WT-G269S and G269S models exhibited moderately prolonged QTc (412 ms for WT-G269S, and 417 ms for G269S), extended T-wave duration and slightly elevated T-wave amplitude. Notice these values fall into the normal QTc range [9]. In contrast, after exercise QTc was significantly prolonged to 478 ms for WT-G269S and 486 ms for G269S, compared with 434 ms in WT. The amplitude of T-wave was not significantly altered.

Similar to APD analysis, the contribution of blunted adrenergic activation of I_{Ks} was quantified. As a result, the contribution of blunted adrenergic activation of I_{Ks} accounted for 24% of QTc prolongation for WT-G269S, and 14% for G269S, which is in concordance with the contributions in the APD prolongations.

4. Discussion and conclusion

Under control conditions with slow pacing rates, the APD of human ventricular action potential is mainly determined by I_{CaL} and the rapid component of delayed

rectifier K^+ current, I_{Kr} [2,4,10]. In accordance with this notion, our simulation data revealed that at rest APD was only mildly prolonged by the WT-G269S and G269S mutation despite the profound positive shift in steady-state activation of I_{Ks} in these mutants. In contrast, the regulatory role of I_{Ks} to APD becomes pronounced after adrenergic stimulation as the increase in I_{Ks} is crucial in offsetting the augmented I_{CaL} to prevent excessive prolongations in APD after adrenergic activation [2]. In our simulations, following the application of ISO, the prolongations in APD by the mutations were roughly doubled in ENDO and EPI cells, and much more pronounced in MCELL. At slow pacing rates, G269S produced EADs, showing a marked prolongation.

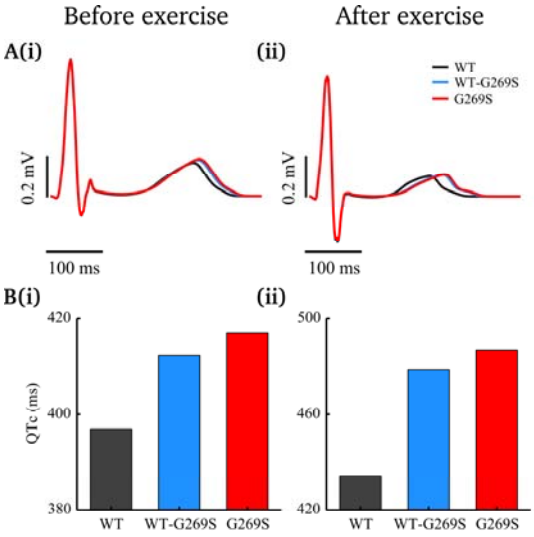

Figure 5. Simulated ECGs showing prolongation in QT interval by the KCNQ1-G269S mutation. A(i) and B(i): control conditions, BCL = 850 ms. A(ii) and B(ii): ISO = 1 μM, BCL = 500 ms. Corrected QT interval (QTc) was evaluated using Bazett's formula [9].

The 1D strand simulations suggest that tissue's VW to genesis of unidirectional conduction was widened and delayed in timing, indicating an increased vulnerability to arrhythmogenesis by the KCNQ1-G269S mutation.

The ECGs obtained from the torso-heart model show that the prolongations in QTc were moderate at rest, but profound after exercise. These findings are consistent with the clinical report [2].

Our simulation data also suggest that the blunted adrenergic activation of I_{Ks} by the mutations also plays a role in the APD and QTc prolongation following the application of ISO, accounting for more than 20% for WT-G269S and 10% for G269S.

In conclusion, our simulations provide mechanistic insights into why the patient with the KCNQ1-G269S mutation remained asymptomatic at rest as the APD prolongation by the mutation was small in the absence of adrenergic stimulation, and that prominent prolonged APD due to loss in repolarisation reserve by reduced basal I_{Ks} current and blunted adrenergic activation underlies the prolonged QT interval after exercise.

Acknowledgements

This work was supported by an EPSRC grant (No. EP/J00958X/1).

References

[1] O-Uchi J, Rice JJ, Ruwald MH, Parks XX, Ronzier E, Moss AJ, Zareba W, Lopes CM. Impaired IKs channel activation by Ca2 +-dependent PKC shows correlation with emotion/arousal-triggered events in LQT1. J Mol Cell Cardiol 2015;79:203–11.

[2] Wu J, Naiki N, Ding W-G, Ohno S, Kato K, Zang W-J, Delisle BP, Matsuura H, Horie M. A Molecular Mechanism for Adrenergic-Induced Long QT Syndrome. J Am Coll Cardiol 2014;63:819–27.

[3] O'Hara T, Rudy Y. Arrhythmia formation in subclinical ("silent") long QT syndrome requires multiple insults: Quantitative mechanistic study using the KCNQ1 mutation Q357R as example. Heart Rhythm Off J Heart Rhythm Soc 2012;9:275–82.

[4] O'Hara T, Virág L, Varró A, Rudy Y. Simulation of the Undiseased Human Cardiac Ventricular Action Potential: Model Formulation and Experimental Validation. PLoS Comput Biol 2011;7:e1002061.

[5] Lee H-C, Rudy Y, Po-Yuan P, Sheu S-H, Chang J-G, Cui J. Modulation of KCNQ1 alternative splicing regulates cardiac IKs and action potential repolarization. Heart Rhythm 2013;10:1220–8.

[6] Adeniran I, McPate MJ, Witchel HJ, Hancox JC, Zhang H. Increased Vulnerability of Human Ventricle to Re-entrant Excitation in hERG-linked Variant 1 Short QT Syndrome. PLoS Comput Biol 2011;7:e1002313.

[7] Alday EAP, Colman MA, Langley P, Butters TD, Higham J, Workman AJ, Hancox JC, Zhang H. A New Algorithm to Diagnose Atrial Ectopic Origin from Multi Lead ECG Systems - Insights from 3D Virtual Human Atria and Torso. PLoS Comput Biol 2015;11:e1004026.

[8] O'Hara T, Rudy Y. Quantitative comparison of cardiac ventricular myocyte electrophysiology and response to drugs in human and nonhuman species. Am J Physiol - Heart Circ Physiol 2012;302:H1023–30.

[9] Johnson JN, Ackerman MJ. QTc: how long is too long? Br J Sports Med 2009;43:657–62.

[10] Jost N, Virág L, Bitay M, Takács J, Lengyel C, Biliczki P, Nagy Z, Bogáts G, Lathrop DA, Papp JG, Varró A. Restricting Excessive Cardiac Action Potential and QT Prolongation A Vital Role for IKs in Human Ventricular Muscle. Circulation 2005;112:1392–9.

Haibo Ni. Haibo.Ni@manchester.ac.uk
Rm 3.08 Schuster Building, the University of Manchester
Oxford Rd, Manchester, UK M13 9PL